

Communication

Compact and Low-Power-Consumption CO Sensor Using a QCL with Intermittent Scanning Technique

Qinduan Zhang ¹, Jie Hu ², Yubin Wei ^{1,*}, Binkai Li ¹, Guancheng Liu ¹, Tingting Zhang ¹, Zhaowei Wang ¹, Weihua Gong ¹ and Tongyu Liu ¹¹ Laser Institute and International School for Optoelectronic Engineering, Qilu University of Technology (Shandong Academy of Sciences), Jinan 250014, China² Shandong Micro-Sensor Photonics Ltd., Jinan 250103, China

* Correspondence: wyb9806@qlu.edu.cn

Abstract: A compact and low-power-consumption gas sensor using a quantum cascade laser (QCL) emitting at 4.6 μm for measurement of carbon monoxide (CO) was proposed and experimentally demonstrated. A compact sensor structure with a physical dimension of $14 \times 10 \times 6.5 \text{ cm}^3$ was designed. A new intermittent scanning technique was used to drive the QCL to reduce the power consumption of the system. In this technique, the power consumption of the sensor is as low as 1.08 W, which is about 75% lower than the conventional direct absorption technology. The stability of the CO sensor was demonstrated by continuously monitoring CO concentration for more than 1 h. In the concentration range of 10 ppm to 500 ppm, the CO sensor exhibited a satisfactory linear response (R-square = 0.9998). With an integration time of 202 s, the minimum detection limit was increased to 4.85 ppb, based on an Allan deviation analysis.

Keywords: low-power-consumption; quantum cascade laser; intermittent scanning technique; CO sensor



Citation: Zhang, Q.; Hu, J.; Wei, Y.; Li, B.; Liu, G.; Zhang, T.; Wang, Z.; Gong, W.; Liu, T. Compact and Low-Power-Consumption CO Sensor Using a QCL with Intermittent Scanning Technique. *Photonics* **2023**, *10*, 95. <https://doi.org/10.3390/photonics10010095>

Received: 6 December 2022

Revised: 10 January 2023

Accepted: 13 January 2023

Published: 15 January 2023



Copyright: © 2023 by the authors. Licensee MDPI, Basel, Switzerland. This article is an open access article distributed under the terms and conditions of the Creative Commons Attribution (CC BY) license (<https://creativecommons.org/licenses/by/4.0/>).

1. Introduction

Carbon monoxide (CO) is a colorless, odorless, and toxic gas formed in the process of human production and life. CO monitoring is essential for coal mine safety [1,2], environmental protection [2], life science [3], and other fields. When CO enters the human body, it combines with hemoglobin in the blood, potentially resulting in poisoning, suffocation, and even mortality. It can also be used as a quantitative marker to assist people in comprehending different production processes. Over the last few decades, thanks to the development of laser technology, CO has been measured by various laser spectroscopy techniques, including tunable diode laser absorption spectroscopy (TDLAS) [4,5], photoacoustic spectroscopy (PAS) [6–8], cavity ring-down spectroscopy (CRDS) [9,10], and cavity-enhanced absorption spectroscopy (CEAS) [11,12].

TDLAS is a low-cost measurement method and has proven to be a practical tool for CO detection in several fields. Vertical-cavity surface-emitting laser (VCSEL) [1,13,14], distributed feedback laser (DFB) [15–18], interband cascade laser (ICL) [19,20], and quantum cascade laser (QCL) [21] are the better excitation laser sources in TDLAS gas detection systems, because they have the characteristics of single frequency emission and narrow linewidth at the CO absorption line. Previously, many CO detection systems based on TDLAS have been reported. For example, Wang et al. [13] reported a TDLAS sensor with a 1.58 μm VCSEL for CO detection, achieving a minimum detection limit of 200 ppm. Cui et al. [16] used a diode laser emitting at 2.33 μm and a 14.5 m multipass gas cell (MGC) for CO detection which achieved a minimum detection limit of 6 ppb at a 48 s averaging time. Ghorbani et al. [20] developed a compact sensor for CO monitoring in the atmosphere and exhaled gas based on a room temperature ICL operating at 4.69 μm . Test results showed that minimum detection limits of 2 ppb for direct absorption spectroscopy and 0.6 ppb for

wavelength modulation spectroscopy can be achieved at 20 s and 10 s integration time, respectively. Dang et al. [21] presented a high-precision CO sensing system, which adopts a continuous wave (CW), high power, distributed feedback QCL with a center wavelength of 4.76 μm together with a mini MGC with the absorption length of 1.6 m, and a minimum detection limit of 200 ppb was achieved with an averaging time of about 114 s.

Compact and low-power-consumption gas sensors using Dy^{3+} sulfide fibers [22,23], mini-multi-pass cell [24], portable low-power laser controller [25], and ICL [26,27] have been reported previously. With the development of ICL and QCL, a wide range of mid-infrared wavelengths can be accessed to cover absorption features of many important molecules such as CO, CO_2 , NH_3 , H_2O , H_2S , and C_2H_2 . The common problems of mid-infrared gas detection systems are large and power intensive. Hence, we have reported an intermittent scanning technique to reduce the size and power consumption of the mid-infrared gas detection system. The QCL emitting at 4.6 μm with output laser power of 9.2 mW is employed as an excitation source. Compared with the conventional direct absorption technology, the intermittent scanning technique reduces the power consumption of the sensor. In addition, it also effectively eliminates the wavelength drift effects in fixed wavelength pulse mode. Experimental results showed that the R-square of linear response was greater than 0.9998, and the minimum detection limit was about 4.85 ppb at the integration time of 202 s.

2. Selection of CO Absorption Lines

Figure 1 depicts the CO absorption lines in the spectral range of 1.5–5 μm according to the HITRAN database [28]. It can be seen from Figure 1 that the CO absorption lines are mainly concentrated near the bands of 1.56, 2.3, and 4.6 μm . At the second overtone band near 1.56 μm , the intensity of the strongest CO absorption line is only about $2.2 \times 10^{-23} \text{ cm}^{-1}(\text{molecule}\cdot\text{cm}^{-2})$. Therefore, it is necessary to use an absorption cell with a long optical path to improve the sensitivity of the CO sensor, which will increase the size and deteriorate the stability of the CO sensor. In the first overtone band near 2.3 μm , the absorption line of methane overlaps with that of CO, which limits the application of the CO sensor in some fields. The mid-infrared QCL provides easy access to the CO fundamental band near 4.6 μm , having about 10^4 and 10^2 times stronger absorption line intensity compared to the overtone bands around 1.56 μm and 2.3 μm . Taking into account the cost and the absorption line intensity, a stronger CO absorption line operating at 4594.99 nm (2176.28 cm^{-1}) is selected in our sensor, and the intensity of this absorption line is $4.34 \times 10^{-19} \text{ cm}^{-1}(\text{molecule}\cdot\text{cm}^{-2})$.

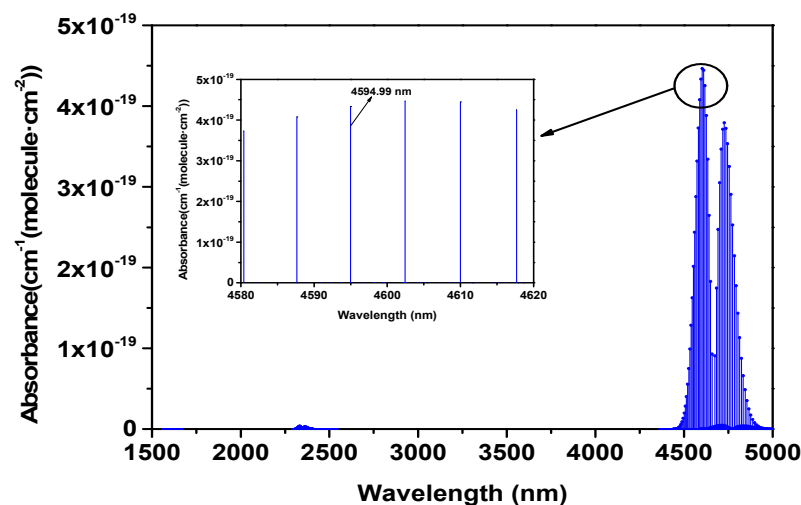


Figure 1. CO absorption lines in the range of 1.5–5 μm .

3. Experimental Configuration

A schematic of the experimental setup for compact and low-power-consumption CO sensor is shown in Figure 2. A QCL (Beijing Institute of Semiconductors, Beijing, China) is used as the laser source, with an output wavelength of approximately $4.6\ \mu\text{m}$. The QCL is mounted on a miniature metal box integrated with a collimating lens and a thermoelectric cooler as shown in Figure 3d. A home-made temperature control circuit is used to tune the temperature of the QCL. The laser driving signals are generated by the ARM (Advanced RISC Machine) to scan the whole gas absorption line. At a temperature of $23\ ^\circ\text{C}$ and a current scan interval of 249–280 mA, an average output power of 9.2 mW is achieved. The laser beam emitted from the QCL is incident into a home-made small gas cell. The small gas cell contains two plane mirrors, which provides an effective optical path of 21 cm, and has a volume of 60 mL. After exiting the gas cell, the laser beam is focused onto an InAsSb detector. The InAsSb detector (AM03120-02-SAMPLE, VIGO System SA, Ozarow Mazowiecki, Poland) converts optical signals into electrical signals. The data processing circuit is used to amplify and filter the electrical signals. Then, the processed signal is collected by ARM for further processing and displayed on the computer. Figure 3a–c shows the photographs of the compact and low-power-consumption CO sensor, the CO sensor has a length of 14 cm, a width of 10 cm, a height of 6.5 cm, which meets the requirements of miniaturization in many fields.

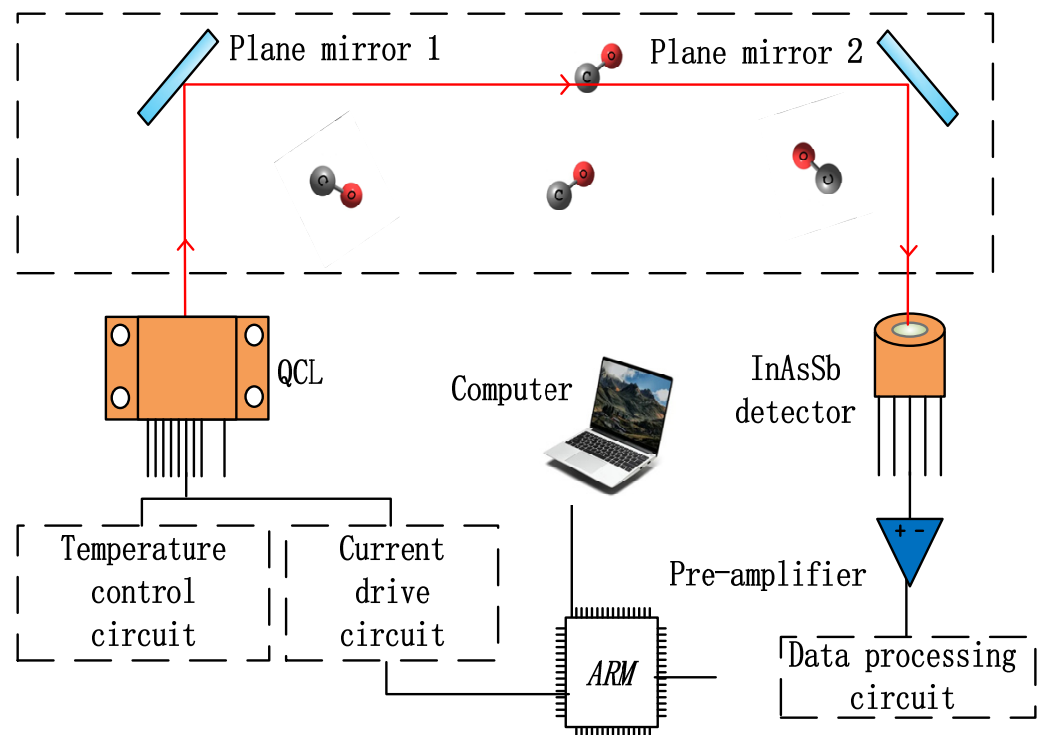


Figure 2. Schematic drawings of the compact and low-power-consumption CO sensor.

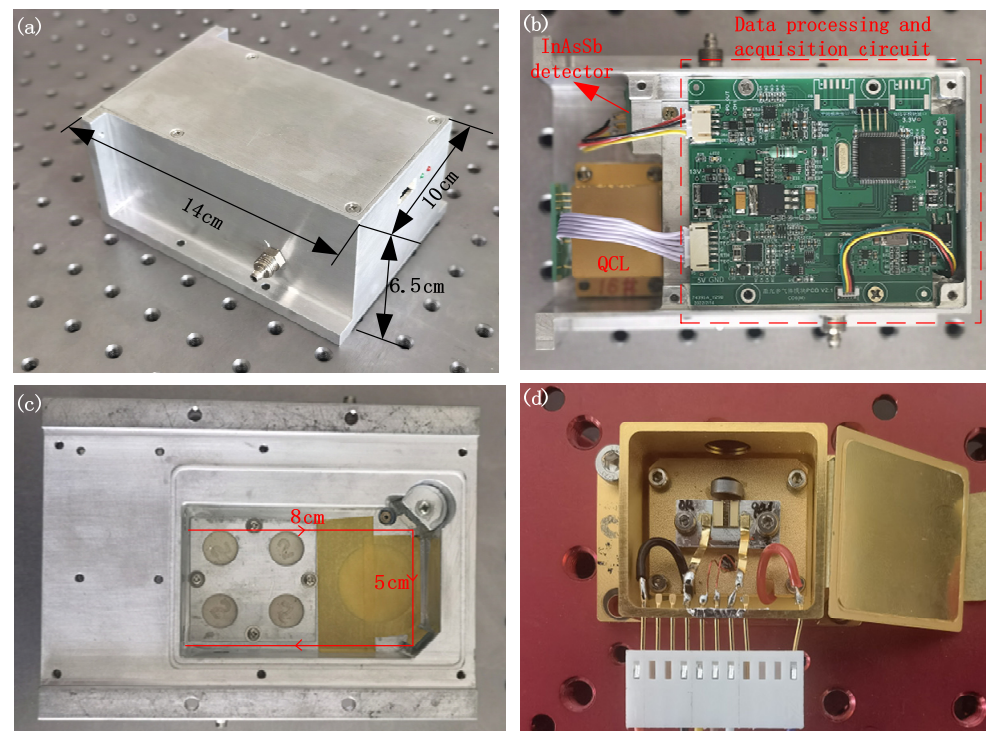


Figure 3. Photographs of (a) the compact and low-power-consumption CO sensor; (b) internal structure of the CO sensor; (c) small gas cell, located on the back of CO sensor; and (d) the QCL.

4. Intermittent Scanning Technique

Common modulation methods for lasers in QCL based gas sensor include fixed wavelength pulse mode [29], conventional direct absorption technology [28], and wavelength modulation spectroscopy [30,31]. In fixed wavelength pulse mode, the output wavelength of the QCL needs to be stabilized at the wavelength of the gas absorption peak. A pulse signal is used to modulate the injection current of the laser as shown in Figure 4a. However, laser wavelength drift caused by external ambient temperature fluctuations is an important factor affecting the accuracy of gas detection system in fixed wavelength pulse mode. Conventional direct absorption technology (see Figure 4b) can reduce the interference of the external ambient temperature on the laser, but the QCL needs to work continuously, resulting in serious heating. Therefore, it is necessary to install a heat dissipation device for the sensor, which increases the power consumption and size of the sensor. Wavelength modulation spectroscopy usually allows better detection accuracy due to reduced 1/f noise [32,33], but it requires higher performance of the signal processing circuit, which will increase the power consumption and cost.

Figure 4c shows an intermittent scanning technique combining pulse mode and conventional direct absorption technology. In this technique, the driving signal consists of “working state T_1 ” and “resting state T_2 ”. When the driving signal is in the “working state T_1 ”, the soft start circuit gradually increases the current signal to make it exceed the laser threshold, and then superimposes the sawtooth wave signal to achieve continuous scanning of the output wavelength. The corresponding driving signal is used to drive the QCL source as shown in Figure 4d. When the “working state T_1 ” is completed, the soft shutdown circuit makes the current signal gradually reduce to zero, and the QCL is in the “resting state T_2 ”, which greatly reduces the power consumption of QCL. The heat generated by the QCL in the “working state T_1 ” can be lost during the “resting state T_2 ”. The duty cycle of the driving signal in the “working state T_1 ” and “resting state T_2 ” can be automatically adjusted and optimized by monitoring the real-time temperature of the QCL, so that the QCL can be kept in a thermally balanced working state. Therefore, the sensor does not need a heat dissipation device, which reduces the power consumption and size

of the sensor. Compared with the conventional direct absorption technology, the power consumption of the sensor in the intermittent scanning technique is reduced by 75%, about 1.08 W.

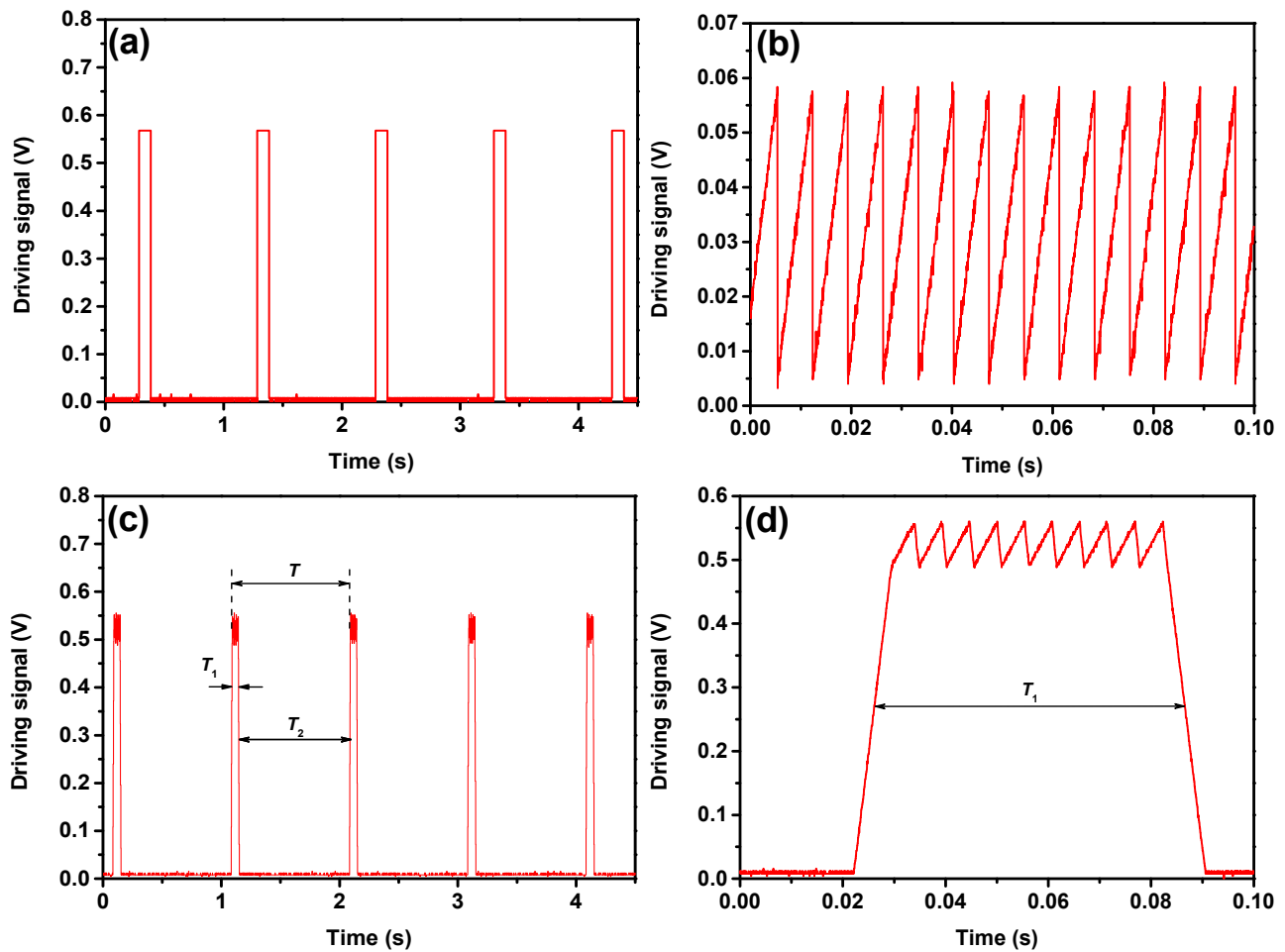


Figure 4. Laser driving signal. (a) Fixed wavelength pulse mode; (b) conventional direct absorption technology; (c) intermittent scanning technique; (d) working state in intermittent scanning technique.

5. Experimental Results

By controlling the flow rate of high precision gas mixing device (RCS 2000-A, Beijing Kingsun Electronics, Beijing, China), different concentrations of the CO/N₂ gas mixture can be accurately obtained. The concentrations of the CO were successively configured to be 10, 20, 50, 100, 200, 350, and 500 ppm. These gases were flowed into the home-made gas cell in turn to verify the response characteristics of our CO sensor. All the measurements were carried out at the normal pressure and room temperature. The absorption signals were measured near the wavelength of 4594.99 nm at different concentrations of CO, as shown in Figure 5.

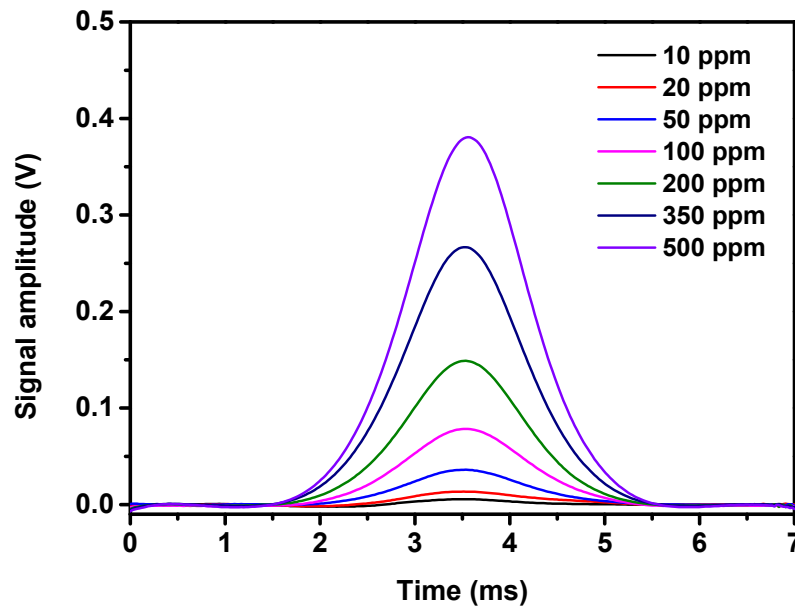


Figure 5. Measured signal amplitude of CO at different concentration levels.

The signal amplitude as a function of CO concentration ranging from 10 ppm to 500 ppm is plotted in Figure 6. The calculated R-square value is 0.9998 in this CO sensor, which indicates that the response signal has an excellent linear response to the CO gas concentration.

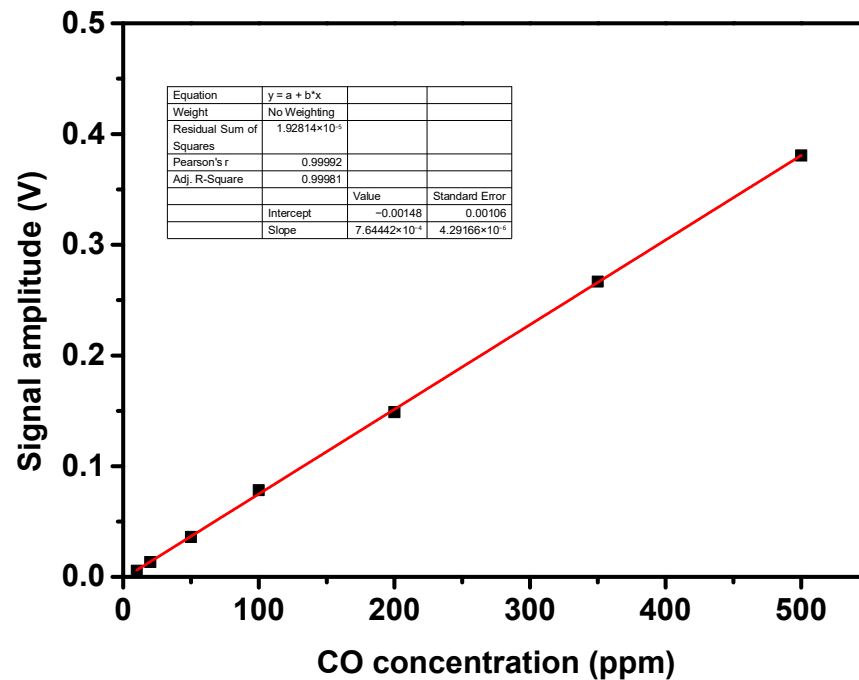


Figure 6. Linear dependence of signal amplitude versus CO gas concentration.

In order to confirm the stability of our CO sensor, a long-term detection experiment of the sensor response to 10 ppm and 500 ppm CO concentration was carried out. Measured signal amplitude changes of CO over 1 h are shown in Figure 7. It is observed that the signal amplitude of CO is comparatively steady during this period. The concentration fluctuation is only about 4 ppm. These measurements show that our sensor can detect CO with high stability. The main reasons for the signal fluctuations include the drifts of the

QCL wavelength and power, the noise caused by the self-made circuit, instability of the detector in long-term operation, optical fringes, etc.

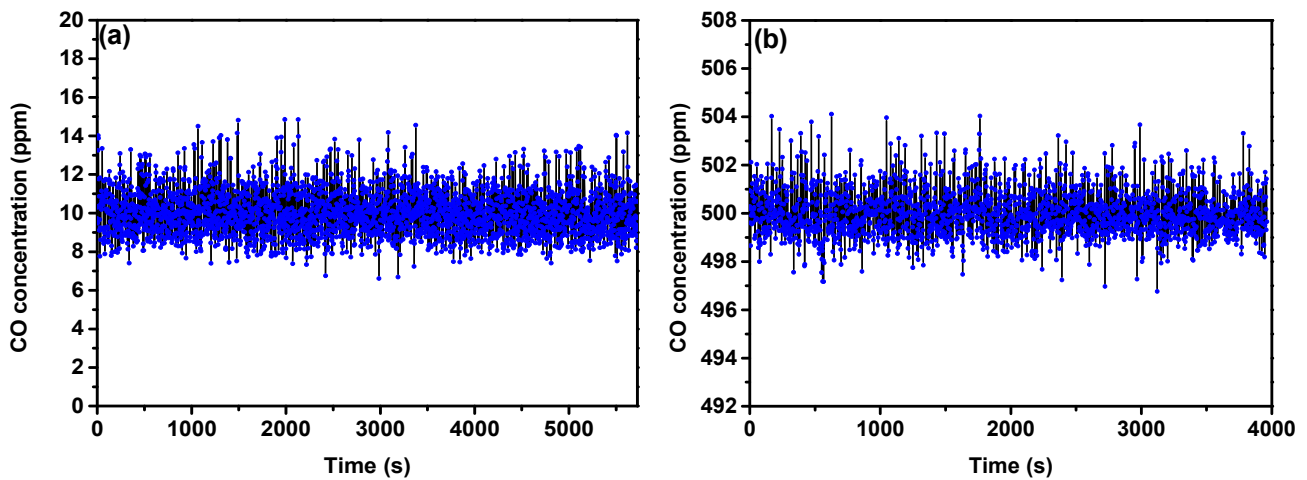


Figure 7. Long-term stability of the compact and low-power-consumption CO sensor (a) 10 ppm CO; (b) 500 ppm CO.

Finally, to evaluate the performance of the compact and low-power-consumption CO sensor, an Allan deviation analysis was computed when 99.9% N₂ gas was injected into the CO sensor. Figure 8 shows the Allan deviation analysis results of the CO sensor, where the integration time varies from 1 s to 200 s. The Allan deviation follows a dependence, which indicates that the main noise of the compact and low-power-consumption CO sensor is white noise [34]. When the integration time is 202 s, a minimum detection limit of 4.85 ppb is achieved.

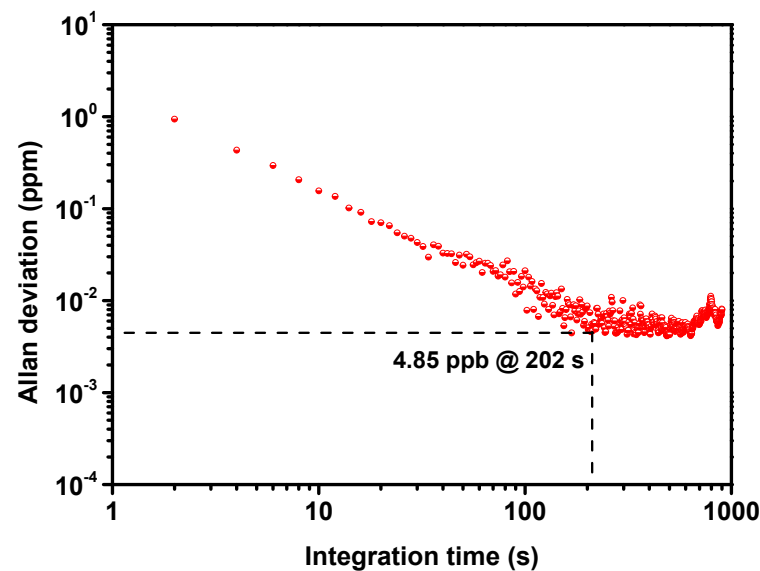


Figure 8. Allan deviation plot for the compact and low power-consumption CO sensor.

6. Discussion

In this work, we developed a TDLAS gas sensor system for a CO analysis by use of a 4.6 μm QCL and intermittent scanning technique. The above experimental results prove the ability of this proposed compact low-power sensor for measurement of CO concentration with high precision. In this sensor, we chose a 4.6 μm QCL as the excitation laser source whose output spectrum range can cover the absorption lines of several gases, such as CO and N₂O [35,36]. Hence, this sensor can be readily employed to detect N₂O by properly

adjusting the driving current and temperature of the laser. Since the TDLAS gas sensor system uses an InAsSb detector with a response wavelength range of 2–5 μm to collect mid-infrared laser, which covers absorption transitions of many different gas species in this wavelength range. Therefore, the TDLAS gas sensor can be easily extended to monitor more industrial harmful gases by replacing the laser source without reducing the detection accuracy of the sensor.

7. Conclusions

In conclusion, we developed and demonstrated a compact and low-power-consumption CO sensor based on the intermittent scanning technique. To demonstrate reliability and long-term stability of the CO sensor, a continuous monitoring of 10 ppm and 500 ppm CO for a period of 1 h was performed. The results showed that the sensor has good stability. The CO linear experimental measurements showed that this CO sensor has a better linear response (R -square = 0.9998) in the concentration range of 10 ppm to 500 ppm. Allan deviation analysis was performed to study the detection accuracy of the CO sensor, and a minimum detection limit of 4.85 ppb was achieved with an integration time of about 202 s. Hence, this CO sensor is suitable for applications in coal mine safety, environmental protection, as well as in life science.

Author Contributions: Methodology, Q.Z.; Software, Q.Z. and J.H.; Validation, Q.Z. and T.Z.; Investigation, Q.Z., B.L. and G.L.; Resources, J.H. and Y.W.; Data curation, Q.Z., Z.W. and W.G.; Writing—original draft preparation, Q.Z.; Writing—review and editing, Q.Z.; Supervision, Y.W. and T.L. All authors have read and agreed to the published version of the manuscript.

Funding: This work was supported by National Key Research and Development Program of China (2021YFB3201905), Natural Science Foundation of Shandong Province (ZR2022QF035), Project of Qilu University of Technology (2022PX010, 2021YY01005), The National Natural Science Foundation of China (62005138), The Major Scientific and Technological Innovation Project of Shandong Province (ZR2020KC012), Project of Jinan (2020GXRC032, 2021GXRC037).

Institutional Review Board Statement: Not applicable.

Informed Consent Statement: Not applicable.

Data Availability Statement: Not applicable.

Conflicts of Interest: The authors declare no conflict of interest.

References

1. Wang, Z.; Li, Y.; Zhang, T.; Hu, J.; Wang, Y.; Wei, Y.; Liu, T.; Sun, T.; Grattan, K.T.V. A Sensitive and Reliable Carbon Monoxide Monitor for Safety-Focused Applications in Coal Mine Using a 2.33- μm Laser Diode. *IEEE Sens. J.* **2019**, *20*, 171–177. [[CrossRef](#)]
2. Yamazoe, N.; Miura, N. Development of gas sensors for environmental protection. *IEEE Trans. Compon. Packag. Manuf. Technol. A* **1995**, *18*, 252–256. [[CrossRef](#)]
3. Chen, C.-C.; Sung, G.-N.; Chen, W.-C.; Kuo, C.-T.; Chue, J.-J.; Wu, C.-M.; Huang, C.-M. A wireless and batteryless intelligent carbon monoxide sensor. *Sensors* **2016**, *16*, 1568. [[CrossRef](#)] [[PubMed](#)]
4. Lewen, Z.; Zhirong, Z.; Qianjin, W.; Pengshuai, S.; Bian, W.; Tao, P.; Hua, X.; Sigrist, M.W. A sensitive carbon monoxide sensor for industrial process control based on laser absorption spectroscopy with a 2.3 μm distributed feedback laser. *Opt. Lasers Eng.* **2022**, *152*, 106950. [[CrossRef](#)]
5. Zhang, T.; Wei, Y.; Li, Y.; Zhao, Y.; Liu, T.; Wang, C. High-resolution fiber carbon monoxide sensing system and its data processing. In Proceedings of the Fourth Asia Pacific Optical Sensors Conference, Wuhan, China, 15–18 October 2013; pp. 82–85.
6. Yin, X.; Wu, H.; Dong, L.; Ma, W.; Zhang, L.; Yin, W.; Xiao, L.; Jia, S.; Tittel, F.K. Ppb-level photoacoustic sensor system for saturation-free CO detection of SF₆ decomposition by use of a 10 W fiber-amplified near-infrared diode laser. *Sens. Actuator B-Chem.* **2019**, *282*, 567–573. [[CrossRef](#)]
7. Qiao, S.; Ma, Y.; He, Y.; Yu, X.; Zhang, Z.; Tittel, F.K. A sensitive carbon monoxide sensor based on photoacoustic spectroscopy with a 2.3 μm mid-infrared high-power laser and enhanced gas absorption. *Sensors* **2019**, *19*, 3202. [[CrossRef](#)] [[PubMed](#)]
8. He, Y.; Ma, Y.; Tong, Y.; Yu, X.; Tittel, F.K. A portable gas sensor for sensitive CO detection based on quartz-enhanced photoacoustic spectroscopy. *Opt. Laser Technol.* **2019**, *115*, 129–133. [[CrossRef](#)]
9. Mondelain, D.; Sala, T.; Kassi, S.; Romanini, D.; Marangoni, M.; Campargue, A. Broadband and highly sensitive comb-assisted cavity ring down spectroscopy of CO near 1.57 μm with sub-MHz frequency accuracy. *J. Quant. Spectrosc. Radiat. Transf.* **2015**, *154*, 35–43. [[CrossRef](#)]

10. Chen, H.; Karion, A.; Rella, C.; Winderlich, J.; Gerbig, C.; Filges, A.; Newberger, T.; Sweeney, C.; Tans, P.P. Accurate measurements of carbon monoxide in humid air using the cavity ring-down spectroscopy (CRDS) technique. *Atmos. Meas. Tech.* **2013**, *6*, 1031–1040. [[CrossRef](#)]
11. Sun, K.; Wang, S.; Sur, R.; Chao, X.; Jeffries, J.B.; Hanson, R.K. Time-resolved in situ detection of CO in a shock tube using cavity-enhanced absorption spectroscopy with a quantum-cascade laser near 4.6 μm . *Opt. Express* **2014**, *22*, 24559–24565. [[CrossRef](#)] [[PubMed](#)]
12. Provencal, R.; Gupta, M.; Owano, T.G.; Baer, D.S.; Ricci, K.N.; O’Keefe, A.; Podolske, J.R. Cavity-enhanced quantum-cascade laser-based instrument for carbon monoxide measurements. *Appl. Opt.* **2005**, *44*, 6712–6717. [[CrossRef](#)] [[PubMed](#)]
13. Wang, F.; Li, N.; Huang, Q.; Yan, J.; Cen, K. Measurements on CO concentration and gas temperature at 1.58 μm with tunable diode laser absorption spectroscopy. In Proceedings of the AIP Conference Proceedings, Macao, China, 1–2 February 2013; pp. 499–508.
14. Sane, A.; Satija, A.; Lucht, R.P.; Gore, J.P. Simultaneous CO concentration and temperature measurements using tunable diode laser absorption spectroscopy near 2.3 μm . *Appl. Phys. B-Lasers Opt.* **2014**, *117*, 7–18. [[CrossRef](#)]
15. Teichert, H.; Fernholz, T.; Ebert, V. Simultaneous in situ measurement of CO, H₂O, and gas temperatures in a full-sized coal-fired power plant by near-infrared diode lasers. *Appl. Opt.* **2003**, *42*, 2043–2051. [[CrossRef](#)] [[PubMed](#)]
16. Cui, R.; Dong, L.; Wu, H.; Li, S.; Zhang, L.; Ma, W.; Yin, W.; Xiao, L.; Jia, S.; Tittel, F.K. Highly sensitive and selective CO sensor using a 2.33 μm diode laser and wavelength modulation spectroscopy. *Opt. Express* **2018**, *26*, 24318–24328. [[CrossRef](#)]
17. Shao, L.; Fang, B.; Zheng, F.; Li, S.; Zhang, L.; Ma, W.; Yin, W.; Xiao, L.; Jia, S.; Tittel, F.K. Simultaneous detection of atmospheric CO and CH₄ based on TDLAS using a single 2.3 μm DFB laser. *Spectrochim. Acta A* **2019**, *222*, 117118. [[CrossRef](#)]
18. Li, C.; Wu, Y.; Qiu, X.; Wei, J.; Deng, L. Pressure-dependent detection of carbon monoxide employing wavelength modulation spectroscopy using a herriott-type cell. *Appl. Spectrosc.* **2017**, *71*, 809–816. [[CrossRef](#)] [[PubMed](#)]
19. Ye, W.; Li, C.; Zheng, C.; Sanchez, N.P.; Gluszek, A.K.; Hudzikowski, A.J.; Dong, L.; Griffin, R.J.; Tittel, F.K. Mid-infrared dual-gas sensor for simultaneous detection of methane and ethane using a single continuous-wave interband cascade laser. *Opt. Express* **2016**, *24*, 16973–16985. [[CrossRef](#)] [[PubMed](#)]
20. Ghorbani, R.; Schmidt, F.M. ICL-based TDLAS sensor for real-time breath gas analysis of carbon monoxide isotopes. *Opt. Express* **2017**, *25*, 12743–12752. [[CrossRef](#)] [[PubMed](#)]
21. Dang, J.; Yu, H.; Sun, Y.; Wang, Y. A CO trace gas detection system based on continuous wave DFB-QCL. *Infrared Phys. Technol.* **2017**, *82*, 183–191. [[CrossRef](#)]
22. Starecki, F.; Charpentier, F.; Doualan, J.; Quetel, L.; Michel, K.; Chahal, R.; Troles, J.; Bureau, B.; Braud, A.; Camy, P.; et al. Mid-IR optical sensor for CO₂ detection based on fluorescence absorbance of Dy³⁺: Ga₅Ge₂₀Sb₁₀S₆₅ fibers. *Sens. Actuator B-Chem.* **2015**, *207*, 518–525. [[CrossRef](#)]
23. Starecki, F.; Morais, S.; Chahal, R.; Boussard-Plédel, C.; Bureau, B.; Palencia, F.; Lecoutre, C.; Garrabos, Y.; Marre, S.; Nazabal, V. IR emitting Dy³⁺ doped chalcogenide fibers for in situ CO₂ monitoring in high pressure microsystems. *Int. J. Greenh. Gas Con.* **2016**, *55*, 36–41. [[CrossRef](#)]
24. Wei, T.; Wu, H.; Dong, L.; Cui, R.; Jia, S. Palm-sized methane TDLAS sensor based on a mini-multi-pass cell and a quartz tuning fork as a thermal detector. *Opt. Express* **2021**, *29*, 12357–12364. [[CrossRef](#)] [[PubMed](#)]
25. Li, N.; Qiu, X.; Wei, Y.; Zhang, E.; Wang, J.; Li, C.; Peng, Y.; Wei, J.; Meng, H.; Wang, G.; et al. A portable low-power integrated current and temperature laser controller for high-sensitivity gas sensor applications. *Rev. Sci. Instrum.* **2018**, *89*, 103103. [[CrossRef](#)] [[PubMed](#)]
26. Dong, L.; Tittel, F.K.; Li, C.; Sanchez, N.P.; Wu, H.; Zheng, C.; Yu, Y.; Sampaolo, A.; Griffin, R.J. Compact TDLAS based sensor design using interband cascade lasers for mid-IR trace gas sensing. *Opt. Express* **2016**, *24*, A528–A535. [[CrossRef](#)] [[PubMed](#)]
27. Dong, L.; Li, C.; Sanchez, N.P.; Gluszek, A.K.; Griffin, R.J.; Tittel, F.K. Compact CH₄ sensor system based on a continuous-wave, low power consumption, room temperature interband cascade laser. *Appl. Phys. Lett.* **2016**, *108*, 011106. [[CrossRef](#)]
28. Gordon, I.; Rothman, L.; Hargreaves, R.; Hashemi, R.; Karlovets, E.; Skinner, F.; Conway, E.; Hill, C.; Kochanov, R.; Tan, Y.; et al. The HITRAN2020 molecular spectroscopic database. *J. Quant. Spectrosc. Radiat. Transf.* **2022**, *277*, 107949. [[CrossRef](#)]
29. Li, L.; Cao, F.; Wang, Y.; Cong, M.; An, Y.; Song, Z.; Guo, S.; Liu, F.; Wang, L. Design and characteristics of quantum cascade laser-based CO detection system. *Sens. Actuator B-Chem.* **2009**, *142*, 33–38. [[CrossRef](#)]
30. Hancock, G.; Van Helden, J.; Peverall, R.; Ritchie, G.A.D.; Walker, R.J. Direct and wavelength modulation spectroscopy using a cw external cavity quantum cascade laser. *Appl. Phys. Lett.* **2009**, *94*, 201110. [[CrossRef](#)]
31. Qiao, S.; Ma, Y.; He, Y.; Patimisco, P.; Sampaolo, A.; Spagnolo, V. Ppt level carbon monoxide detection based on light-induced thermoelastic spectroscopy exploring custom quartz tuning forks and a mid-infrared QCL. *Opt. Express* **2021**, *29*, 25100–25108. [[CrossRef](#)]
32. Vanderover, J.; Wang, W.; Oehlschlaeger, M. A carbon monoxide and thermometry sensor based on mid-IR quantum-cascade laser wavelength-modulation absorption spectroscopy. *Appl. Phys. B-Lasers Opt.* **2011**, *103*, 959–966. [[CrossRef](#)]
33. Li, J.; Deng, H.; Sun, J.; Yu, B.; Fischer, H. Simultaneous atmospheric CO, N₂O and H₂O detection using a single quantum cascade laser sensor based on dual-spectroscopy techniques. *Sens. Actuator B-Chem.* **2016**, *231*, 723–732. [[CrossRef](#)]
34. Werle, P.O.; Mücke, R.; Slemr, F. The limits of signal averaging in atmospheric trace-gas monitoring by tunable diode-laser absorption spectroscopy (TDLAS). *Appl. Phys. B-Lasers Opt.* **1993**, *57*, 131–139. [[CrossRef](#)]

35. Li, J.; Parchatka, U.; Fischer, H. Development of field-deployable QCL sensor for simultaneous detection of ambient N₂O and CO. *Sens. Actuator B-Chem.* **2013**, *182*, 659–667. [[CrossRef](#)]
36. Tao, L.; Sun, K.; Khan, M.A.; Miller, D.J.; Zondlo, M.A. Compact and portable open-path sensor for simultaneous measurements of atmospheric N₂O and CO using a quantum cascade laser. *Opt. Express* **2012**, *20*, 28106–28118. [[CrossRef](#)] [[PubMed](#)]

Disclaimer/Publisher’s Note: The statements, opinions and data contained in all publications are solely those of the individual author(s) and contributor(s) and not of MDPI and/or the editor(s). MDPI and/or the editor(s) disclaim responsibility for any injury to people or property resulting from any ideas, methods, instructions or products referred to in the content.